

Shape-influenced non-reciprocal transport of magnetic skyrmions in nanoscale channel

Jie-Yao Chen(陈杰尧), Jia Luo(罗佳), Geng-Xin Hu(胡更新), Jun-Lin Wang(王君林), Guan-Qi Li(李冠祺), Zhen-Dong Chen(陈振东), Xian-Yang Lu(陆显扬), Guo-Ping Zhao(赵国平), Yuan Liu(刘远), Jing Wu(吴竞), and Yong-Bing Xu(徐永兵)

Citation: Chin. Phys. B, 2024, 33 (**7**): 077505. DOI: 10.1088/1674-1056/ad34c7
Journal homepage: http://cpb.iphy.ac.cn; http://iopscience.iop.org/cpb

What follows is a list of articles you may be interested in

Creation and annihilation of artificial magnetic skyrmions with the electric field

Jun Cheng(程军), Liang Sun(孙亮), Yike Zhang(张一可), Tongzhou Ji(吉同舟), Rongxing Cao(曹荣幸), Bingfeng Miao(缪冰锋), Yonggang Zhao(赵永刚), and Haifeng Ding(丁海峰)
Chin. Phys. B, 2024, 33 (**3**): 037501. DOI: 10.1088/1674-1056/ad188f

Oscillation of Dzyaloshinskii-Moriya interaction driven by weak electric fields

Runze Chen(陈润泽), Anni Cao(曹安妮), Xinran Wang(王馨苒), Yang Liu(柳洋), Hongxin Yang(杨洪新), and Weisheng Zhao(赵巍胜)
Chin. Phys. B, 2024, 33 (**2**): 027501. DOI: 10.1088/1674-1056/ad0f85

Tunable dispersion relations manipulated by strain in skyrmion-based magnonic crystals

Zhao-Nian Jin(金兆年), Xuan-Lin He(何宣霖), Chao Yu(于超), Henan Fang(方贺男), Lin Chen(陈琳), and Zhi-Kuo Tao(陶志阔)
Chin. Phys. B, 2024, 33 (**1**): 017501. DOI: 10.1088/1674-1056/acf03c

Magnonic band-pass and band-stop filters with structurally modulated waveguides

Lai-He Feng(冯来和), Mang-Yuan Ma(马莽原), Zhi-Hua Liu(刘智华), Kai-Le Xie(解凯乐), and Fu-Sheng Ma(马付胜)
Chin. Phys. B, 2023, 32 (**6**): 067503. DOI: 10.1088/1674-1056/ac8afb

Gate-voltage control of alternating-current-driven skyrmion propagation in ferromagnetic nanotrack devices

Xin-Yi Cai(蔡心怡), Zhi-Hua Chen(陈志华), Hang-Xiao Yang(杨航霄), Xin-Yan He(何鑫岩), Zhen-Zhen Chen(陈珍珍), Ming-Min Zhu(朱明敏), Yang Qiu(邱阳), Guo-Liang Yu(郁国良), and Hao-Miao Zhou(周浩淼)
Chin. Phys. B, 2023, 32 (**6**): 067502. DOI: 10.1088/1674-1056/acb420

Shape-influenced non-reciprocal transport of magnetic skyrmions in nanoscale channel

Jie-Yao Chen(陈杰尧)[1,2,†], Jia Luo(罗佳)[3,†], Geng-Xin Hu(胡更新)[4], Jun-Lin Wang(王君林)[1,2,‡], Guan-Qi Li(李冠祺)[1,2], Zhen-Dong Chen(陈振东)[1,2], Xian-Yang Lu(陆显扬)[4], Guo-Ping Zhao(赵国平)[3,§], Yuan Liu(刘远)[1], Jing Wu(吴竞)[1,2], and Yong-Bing Xu(徐永兵)[1,2,¶]

[1] *School of Integrated Circuits, Guangdong University of Technology, Guangzhou* 510006, *China*
[2] *School of Physics, Engineering and Technology, University of York, York YO*10 5*DD, United Kingdom*
[3] *College of Physics and Electronic Engineering, Sichuan Normal University, Chengdu* 610068, *China*
[4] *Jiangsu Provincial Key Laboratory of Advanced Photonic and Electronic Materials, School of Electronic Science and Engineering, Nanjing University, Nanjing* 210093, *China*

(Received 25 December 2023; revised manuscript received 6 March 2024; accepted manuscript online 18 March 2024)

Skyrmions, with their vortex-like structures and inherent topological protection, play a pivotal role in developing innovative low-power memory and logic devices. The efficient generation and control of skyrmions in geometrically confined systems are crucial for the development of skyrmion-based spintronic devices. In this study, we focus on investigating the non-reciprocal transport behavior of skyrmions and their interactions with boundaries of various shapes. The shape of the notch structure in the nanotrack significantly affects the dynamic behavior of magnetic skyrmions. Through micromagnetic simulation, the non-reciprocal transport properties of skyrmions in nanowires with different notch structures are investigated in this work.

Keywords: skyrmion, micromagnetic simulation, racetrack memory

PACS: 75.78.Cd, 85.75.–d, 12.39.Dc **DOI:** 10.1088/1674-1056/ad34c7

1. Introduction

With the continuous development of information technology, traditional storage methods have proven insufficient to meet the demands for both large storage capacity and high-speed performance. Therefore, there is an urgent need for storage technologies that can have high-efficiency performance. Among these solutions, novel high-performance storage approaches, such as magnetic domain walls and magnetic skyrmions based racetrack memory, have demonstrated their potential applications in the information industry.[1–4]

These technologies offer extraordinary potential for low-power memory and logic devices, enabling efficient information storage and computing. Magnetic skyrmion is a vortex-like nonlinear spin structure that exhibits quasi-particle characteristic, and inherent topological protection.[5–7] Since the first experiment observation of the magnetic skyrmions in magnetic materials,[6] their remarkable stability, low energy consumption, and nanoscale-size have promoted their application research in spintronic devices.[2,8–11]

The generation, manipulation, and structural evolution of skyrmions can be controlled through various means such as current, lasers, spin waves, and electric fields.[3,12–19] The skyrmion signal in the nanodevice can be detected by the magnetic tunnelling junction detector and topological Hall effect measurement.[20–22] The rich dynamical features and physical effects of magnetic skyrmions possess significant potentials for diverse applications. In recent years, electronic information devices have been proposed based on magnetic skyrmions, including skyrmion racetrack memory, skyrmion nano-oscillators, skyrmion artificial neurons, and stochastic computing devices.[10,11,23–25] These magnetic skyrmion-based devices have smaller sizes, higher integration densities and lower operational energy consumption than previous domain-based devices. These advantages make integrated magnetic skyrmion devices a promising candidate for the next generation of information storage and computational units.

The efficient generation and control of skyrmions in geometrically confined systems are important in developing skyrmion-based spintronic devices. In a geometrically confined system, the stability and dynamics of skyrmions are influenced by boundary effects, inter-skyrmion interactions, and the skyrmion Hall effect. Therefore, before the application of skyrmion-based spintronic devices, it is necessary to address these influences. Currently, there are only limited studies of controlling the unidirectional motion of skyrmions in confined systems, such as using voltage controlled magnetic anisotropy to realize unidirectional motion of skyrmions.[26–28] Therefore, the thermal effects in the device

[†]These authors contributed equally to this work.
[‡]Corresponding author. E-mail: junlin.wang@gdut.edu.cn
[§]Corresponding author. E-mail: zhaogp@uestc.edu.cn
[¶]Corresponding author. E-mail: yongbing.xu@york.ac.uk

© 2024 Chinese Physical Society and IOP Publishing Ltd

can weaken the performance of voltage-controlled skyrmion non-reciprocal transport devices, such as reducing the effective magnetic anisotropy and leading to the failure of voltage control, as well as causing skyrmion Brownian motion and reducing the stability of skyrmions in nanowires.[28–31] Skyrmions still hold great potential ability to achieve complex logic functionalities and combine storage-computation capabilities.[23–28]

In this work, we focus on investigating the non-reciprocal transport behavior of skyrmions and their interactions with boundaries of different notch structures. Through micromagnetic simulation, we explore the non-reciprocal transport properties of skyrmions with different notch structures. Previous research has mainly concentrated on uniform-shaped notches, while this work systematically examines the transport characteristics of skyrmions under different notch conditions by adjusting shapes of notch structure in nano-channels. The schematic of the magnetic nanotrack with a notch structure is given in Fig. 1(a). The findings of this study will contribute to a better understanding of the non-reciprocal transport behavior of skyrmions and their interactions with boundaries, thereby offering crucial theoretical support for the application of skyrmions in novel storage or logic devices. These results hold the potential to advance the field of spintronic in-memory computing devices.

2. Method

In this study, micromagnetic simulations of skyrmion motion are conducted by using Mumax3 software. Mumax3 is a GPU-based micromagnetic simulation software capable of efficiently handling large-scale magnetic problems. We construct a simulation model consisting of an ultrathin ferromagnetic nanochannel with dimensions of 500 nm×80 nm×1.2 nm. The size of the simulation unit cells within the model is set to 2 nm×2 nm×1.2 nm. The simulation is based on the Landau–Lifshitz–Gilbert (LLG) equation, by combining spin–orbit torque. The equation is given as follows:

$$\frac{\mathrm{d}m}{\mathrm{d}t} = -\gamma_0 m \times H_{\mathrm{eff}} + \alpha\left(m \times \frac{\mathrm{d}m}{\mathrm{d}t}\right) - um \times \left(m \times m_{\mathrm{p}}\right). \tag{1}$$

In this equation, m represents the reduced magnetization, denoted as M/M_{S}, with M_{S} being the saturation magnetization; γ_0 denotes the gyromagnetic ratio; α is the damping coefficient; H_{eff} represents the effective field, which includes the contributions from Heisenberg exchange, Dzyaloshinskii–Moriya interaction (DMI), magnetic anisotropy, and the demagnetization field; u can be defined as $\gamma_0 \hbar j P/(2de\mu_0 M_{\mathrm{S}})$, where $\hbar$ is the reduced Planck constant, j is the injection current density, $P = 0.08$ is the spin Hall angle for the spin–orbit torque;[3] e is the electron charge; μ_0 is the vacuum permeability constant, and d is the thickness of the magnetic nanotrack, p is the direction of the spin polarization which is equal to $-\hat{y}$. The parameters of the magnetic material are adopted from Ref. [3]. The values are assigned as follows: saturation magnetization M_{S} is set to 580 kA·m^{-1}, damping coefficient α is 0.3, DMI constant D is 3 mJ·m^{-2}, and exchange constant A is 15 pJ·m^{-1}, and magnetic anisotropy constant K is 0.8 MJ/m^3.[3]

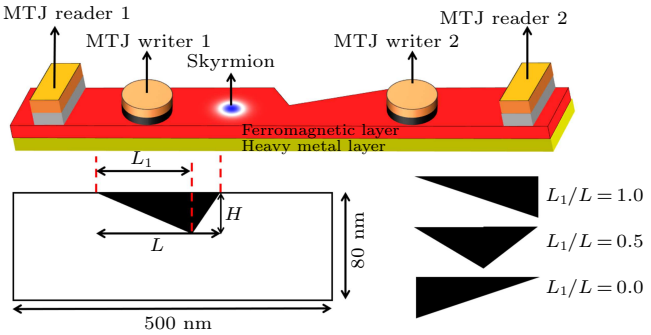


Fig. 1. (a) Schematic diagram of magnetic nanotrack with notch structure with a size of 500 nm×80 nm in size and (b) definitions of different notch structure shapes.

The shape of the notch structure in the model is defined by the following parameters which are given in Fig. 1(b): H represents the depth of the defect, L_1 denotes the shape of the notch, defined by the distance from the lowest point (bottom point) of the notch to the left boundary, while L is the total length of the defect structure. In the simulation, by adjusting the sizes of H and L_1, notches of different shapes can be obtained, and the L is set to 80 nm. The initial position of the magnetic skyrmion is 50 nm away from the left side of the system.

3. Results and discussion

3.1. Current-driven magnetic skyrmion dynamics in nanotrack without notch structure

By studying the motion of skyrmions driven by current in the absence of notches, the dynamics behavior of skyrmions is analyzed in order to determine the appropriate range of driving current for subsequent research. It is observed that the larger the current, the greater the Magnus force is experienced by the skyrmions, resulting in greater longitudinal acceleration. Under sufficiently high current conditions, the longitudinal velocity induced by the Magnus force far exceeds the horizontal velocity under polarized current drive, causing the trajectory of the skyrmion to exhibit a significant inclination. As the skyrmion rapidly moves to the upper boundary, it experiences further repulsion from the boundary. When the boundary repulsion balances with the Magnus force, the skyrmion, due to its strong topological protection, can maintain its structural stability and continue to move horizontally. However, excessive driving current can bring the skyrmion too close to the

boundary, exceeding the critical value of topological protection and leading to the annihilation of the skyrmion. Under the drive of current in the $+x$ direction, the skyrmion moves within the designated nanochannel. When the driving current intensity j is less than 50 MA·cm^{-2} but greater than 10 MA·cm^{-2}, a more effective realization of the passability of skyrmions is achieved.

3.2. Current-driven magnetic skyrmion dynamics in nanotrack with different notch shapes

The motion trajectory of skyrmions at $j = 50$ MA·cm^{-2}, with a notch depth of 22 nm and varying bottom point positions is investigated. Due to the edge force from the shape anisotropy, the notch structure at the edge of the nanotrack will affect the dynamics behaviour of magnetic skyrmion in the constrained system. The depiction of the trajectory of a skyrmion propelled by an electric current is illustrated in Fig. 2.

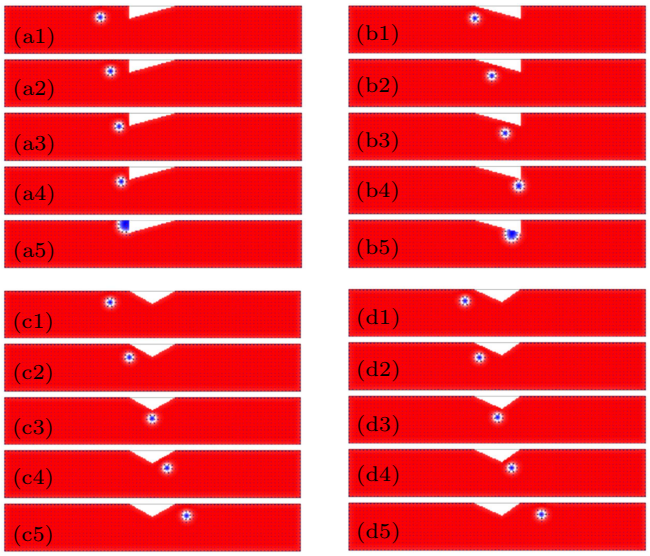


Fig. 2. Spin configuration of skyrmion motion in nanotracks with different notch structures: (a) $L_1/L = 0.0$ and $H = 22$ nm, (b) $L_1/L = 1.0$ and $H = 22$ nm, (c) $L_1/L = 0.5$ and $H = 22$ nm, and (d) $L_1/L = 0.6$ and $H = 22$ nm.

When the bottom point angle of the notch is smaller, the skyrmion is more likely to pinned or disrupted at the notch structure. As shown in Figs. 2(a) and 2(b), where the skyrmions are disrupted by the notch structure during motion. In such cases, the magnus force at the notch boundary becomes higher, making skyrmions difficult to pass through the bottom point of the notch, thereby restricting their motion. The interaction between the skyrmion and the notch structure can be approximately considered as the interaction between the skyrmion and the edge of the nanotrack. Reducing the width of the nanotrack will reduce the stability of the skyrmion in the system.[2,32] However, when the shape of the notch is close to a middle position (i.e., L_1 is close to $0.5L$ and $0.6L$), it is easier for skyrmions to move from left to right when passing through the notch. This is because when the bottom point of the notch is near the midpoint, the repulsive force on magnetic skyrmions is lower, making it easier to cross the notch. It is crucial to note that the influence of notch geometry on skyrmions is attributed to changes in the potential energy gradient. The potential energy gradient at the notch's bottom significantly increases when the bottom angle is small, making it more difficult for the skyrmion to traverse the notch area. Therefore, the shape and position of the notch play a crucial role in the transmission of skyrmions. By optimizing the design of the notch, the nonreciprocity of skyrmions can be made more pronounced.

3.3. Current-driven magnetic skyrmion dynamics in nanotrack with different notch depths

The dynamics behaviors of skyrmion motion in a nanotrack with different values of depth H of the notch structure are studied. The driven current density is assumed to be $j = 50$ MA·cm^{-2}. The trajectories of magnetic skyrmion motion versus depth of notch structure varying from 12 nm to 22 nm are given in Figs. 3(a)–3(d). When the notch depth is 12 nm, the skyrmions can pass through the sloped notch almost at this time, and the change in the slope of the notch mainly causes the lowest point of the trajectory to have a tendency to shift to the right. When the notch depth is 14 nm, it is known from the motion phase diagram that there are conditions under which skyrmions cannot pass through the notch, and from the motion trajectory images of skyrmions in notches with depths of 18 nm and 22 nm, it can be concluded that the larger the depth, the easier it is for skyrmions to be intercepted.

In addition, it is also found that the notch has a significant symmetrical effect on the obstruction of skyrmions. Through the study of notches with a certain depth and varying bottom points, it is found that the motion trajectories of skyrmions with notch bottom point positions at $L_1/L = 0.4$, $L_1/L = 0.6$, $L_1/L = 0.8$ exhibit obvious symmetry as shown in Fig. 3. This phenomenon better illustrates the effects of boundary repulsion and Magnus force on skyrmions near the notch. In addition to finding the symmetry of skyrmion's motion trajectories at bottom point symmetric to $L_1/L = 0.5$, it is found that at different depths, the closer the notch is to the bottom point $L_1/L = 0.5$, the easier it is for skyrmions to move forward through the notch structure area.

Besides, we use the Cartesian coordinate system, in which the x axis, y axis, and z axis are along the height direction, width direction, and thickness direction of the track, respectively. The skyrmion dynamics is well described by using the Thiele equation as follows:[33–35]

$$\boldsymbol{G} \times \boldsymbol{v} + \alpha \boldsymbol{D}_{\text{diss}} \cdot \boldsymbol{v} + \boldsymbol{F}_j + \boldsymbol{F}_{\text{b}} = 0. \tag{2}$$

The first term on the left-hand side in Eq. (2) is the Magnus force with the gyrovector $\boldsymbol{G} = (4\pi Q \mu M_{\text{S}} d/\gamma)\ \boldsymbol{e}_z$. It can be found that the Magnus force is proportional to the topological

charge Q, which is an integer that reflects the number of times the spin direction wraps the unit sphere and expressed as

$$Q = \frac{1}{4\pi}\int (\boldsymbol{m}\cdot(\partial_x \boldsymbol{m}\times\partial_y \boldsymbol{m}))\,\mathrm{d}x\mathrm{d}y, \tag{3}$$

where the number of topologies Q is ±1 for an isolated FM skyrmion. In Eq. (2), the second term describes the dissipative force, in which the dissipation tensor $\boldsymbol{D}_{\rm diss}$ is given by $\boldsymbol{D}_{\rm diss} = (\mu_0 M_{\rm S}\tau/\gamma)\begin{pmatrix} D_{\rm diss} & 0 \\ 0 & D_{\rm diss}\end{pmatrix}$ with $D_{\rm diss} = \int(\partial_x \boldsymbol{m}\cdot\partial_x \boldsymbol{m})\,\mathrm{d}x\mathrm{d}y$. The $\boldsymbol{F}_j$ is the current-induced force that can be written as $\boldsymbol{F}_j = (\mu_0 M_{\rm S} d/\gamma)u\begin{pmatrix} I_x \\ I_y\end{pmatrix}$ with $I_i = \int((\boldsymbol{m}\times\boldsymbol{m}_{\rm p})\cdot\partial_i \boldsymbol{m})\,\mathrm{d}x\mathrm{d}y$. For a stable skyrmion, the boundary force $\boldsymbol{F}_{\rm b}$ is 0 in an infinite film and is opposite to the Magnus force at the boundary. Further, we assume that the current is in the x direction and solve the Thiele equation to obtain the velocity equation of skyrmion. For $\boldsymbol{F}_{\rm b} = 0$, the skyrmion velocity can be expressed as

$$\begin{aligned} v_x &= -\frac{\alpha I_x D_{\rm diss}}{(4\pi Q)^2 + (\alpha D_{\rm diss})^2}u, \\ v_y &= -\frac{4\pi Q I_x}{(4\pi Q)^2 + (\alpha D_{\rm diss})^2}u, \end{aligned} \tag{4}$$

where v_x and v_y represent the velocity component in the x direction and the y direction, respectively. For $\boldsymbol{F}_{\rm b} = -\boldsymbol{G}\times\boldsymbol{v}$, the skyrmion velocity can be expressed as

$$v = v_x = -\frac{I_x}{\alpha D_{\rm diss}}u. \tag{5}$$

There v_x and v_y represent the velocity component in the direction of x and y, respectively. According to Ref. [33], the $D_{\rm diss}$ and I_x in Eqs. (4) and (5) can be approximated as

$$D_{\rm diss} \approx 2\pi\left(\frac{R}{\sqrt{A/K}} + \frac{\sqrt{A/K}}{R}\right)$$

and $I_x \approx \pi^2 R$, where R is the radius of the skyrmion, the symbol A represents the non-uniform exchange constant, K denotes the perpendicular anisotropy, and D refers to the Dzyaloshinskii–Moriya interaction (DMI). The R is related to the material parameters and boundary, where the larger the current, the closer the skyrmion will be to the boundary, so the smaller its radius will be. We simulate the dynamic behavior of skyrmion in unbounded and bounded tracks respectively, where when the current increases from 0 to 80 MA/cm^2, the radius of the skyrmion will decrease from 7.3 nm to 5 nm. We assume that R changes uniformly with the current in this process. We can obtain the velocity of skyrmion, where the simulations accord well with our analytical results as shown in Fig. 4(a).

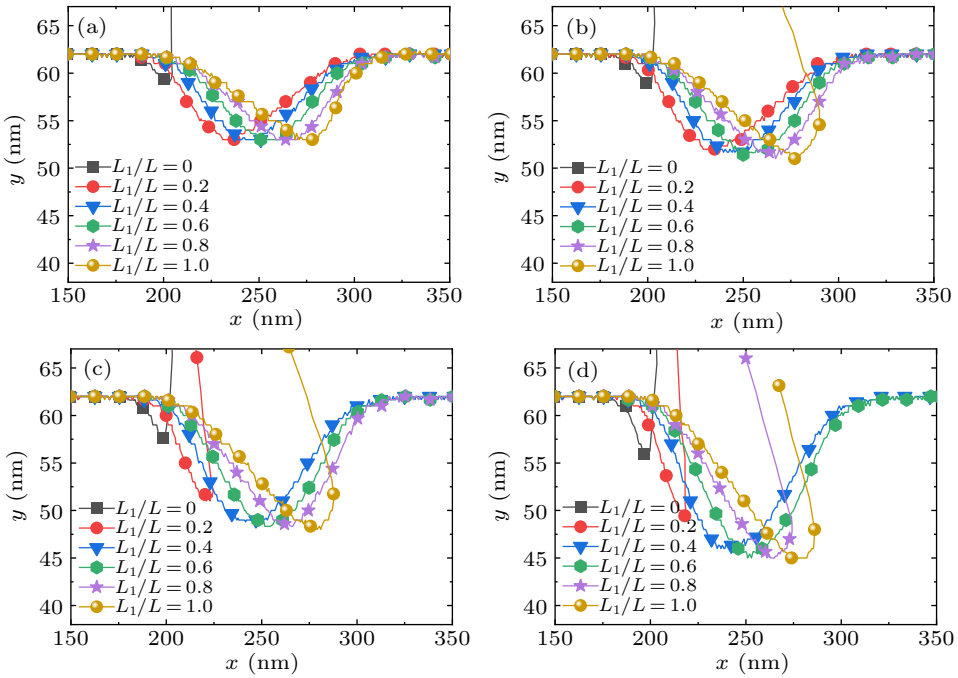


Fig. 3. Trajectories of skyrmion motion in nanotracks with depth H = 12 nm (a), 14 nm (b), 18 nm (c), and 22 nm (d), with driven current density being j = 50 MA·cm^{-2}.

Our simulations show that the Thiele equation is suitable for precise quantitative analysis of the skyrmion's motion and state before encountering the notch. However, once the skyrmion encounters the asymmetric notch structure, neither the Thiele equation nor current theories could accurately predict the skyrmion's motion.[32] Only limited qualitative analysis can be conducted. This limitation arises from the fact that the Thiele equation is designed to study the motion of a skyrmion in a stable state, and the physical state of a skyrmion after encountering a notch is inherently unstable. In addition, we calculate the dependence of skyrmion diameter on nanowire width through micromagnetic simulations. As illus-

trated in Fig. 4(b), the skyrmion size decreases when the width is less than 60 nm. Comparing this with the result shown in Fig. 5 indicates that the increased notch depth can be explained as corresponding nanowire with a reduced width, which in turn affects the skyrmion size and its passability.

3.4. Non-reciprocal transport of magnetic skyrmion in nanotrack with notch structure

The influence of notches on skyrmions is mainly reflected in the adjustment of the balance between boundary repulsion and Magnus force. By modifying the shape of the notch, skyrmions can be made closer to the boundary when passing through the notch, thereby obtaining greater boundary repulsion to balance with the Magnus force. Figure 5 shows that when the shape of the notch is too steep, skyrmions come too close to the boundary, and their topological protection is insufficient to maintain the stability of their topological structure, resulting in the damage to structure. Additionally, such an adjustment can also be realized by modifying the current magnitude. When the current is smaller, the Magnus force on the skyrmions can be reduced, allowing the skyrmions to more easily maintain the stability of their topological structure by moving away from the boundary.

When a skyrmion is driven in the opposite direction, it will exhibit a downward skyrmion Hall effect due to the use of current in the opposite polarization direction. Therefore, for the same notch shape, when skyrmions are driven in the opposite direction, they will quickly move downward close to the boundary, and their motion state is hardly affected by the notch.

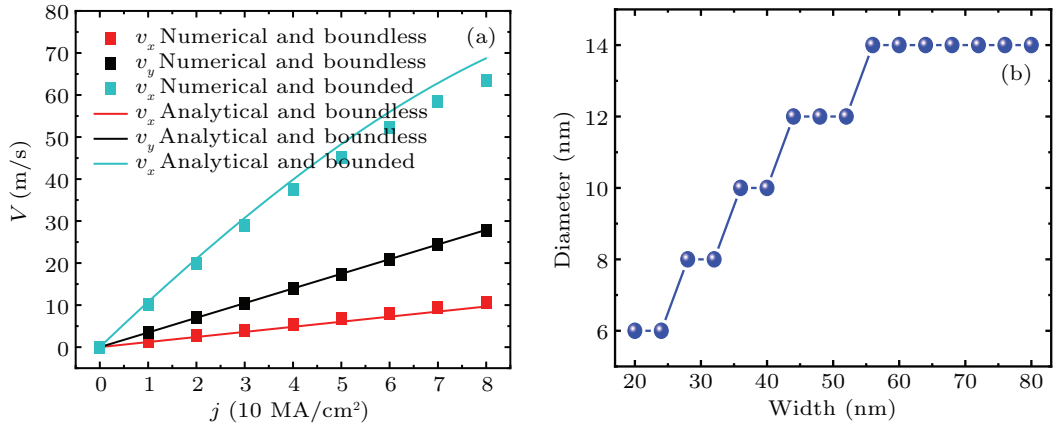


Fig. 4. (a) Plots of skyrmion's velocity versus current. The lines and points are analytical and numerical results, respectively. Red and black represent the results without boundaries, and blue represents the results with boundaries.[33–35] (b) Plot of skyrmion diameter versus width of nanowires.

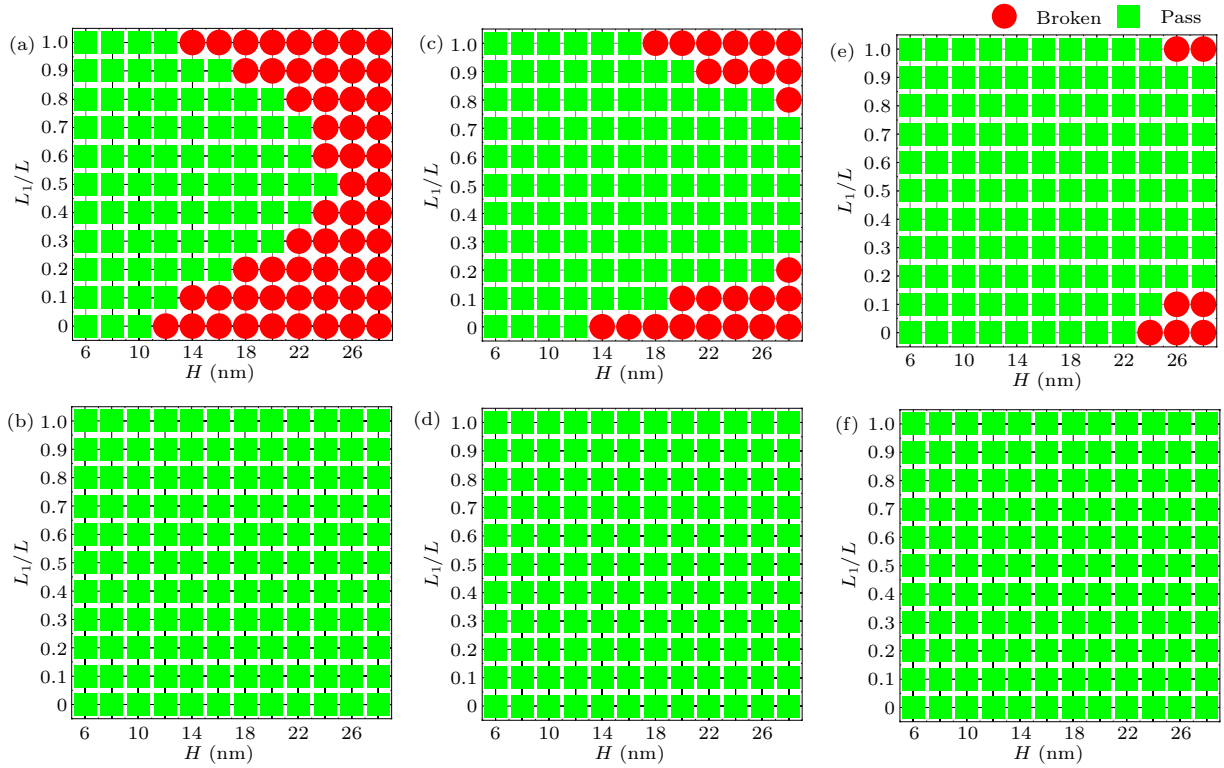


Fig. 5. Skyrmion non-reciprocal transport diagrams, showing ((a), (c), (e)) the forward motion of skyrmions, ((b), (d), (f)) the reverse motion of skyrmions, with driving current magnitude being ((a), (b)) 50 MA·cm^{-2}, ((c), (d)) 40 MA·cm^{-2}, and ((e), (f)) 30 MA·cm^{-2}.

Thus, a construction idea for a skyrmion diode can be proposed: by creating suitable defect shapes in the nanochannel and driving them with appropriate polarized current, skyrmion can exhibit characteristics of not passing in the forward direction and passing in the reverse direction. The phase diagram of the notch structure-induced skyrmon non-reciprocal behavior is given in Fig. 5.

The shape of the defect can vary within a certain range, and the magnitude of the polarization current also satisfies a certain range to achieve this unidirectional passability. This indicates that such a skyrmion diode has a relatively stable non-reciprocal transport window, providing precision redundancy for manufacturing actual devices. At the same time, such a skyrmion diode also has adjustable unidirectional passability. When the current is relatively small, non-reciprocal transport disappears, indicating that it can pass in both directions; and when the current is relatively large, it cannot pass in any direction. This skyrmion diode has richer dynamic properties than traditional MOS structure.

4. Conclusions

By controlling the shape and depth of the notch, we can observe the non-reciprocal transport properties of skyrmions beneath the notch, and such a non-reciprocal transport has a relatively large window, which is conducive to precision control in the actual device manufacturing process. Moreover, such a non-reciprocal transport demonstrates a correlation with the magnitude of polarized current, thereby endowing the skyrmion diode derived from this principle with richer dynamic properties. The obtainment of such a non-reciprocal transport is mainly due to the relatively strong topological protection of skyrmions and the symmetric skyrmion Hall effect. In addition, the idea of a skyrmion channel inhibitor is also proposed. Such a skyrmion inhibitor can control the passage or blocking of skyrmions by regulating the magnitude of the current. This device can be used in information storage to detect whether the output results of the previous stage circuit meet the conditions. In summary, the simulation results demonstrate theinfluence of the notch on the motion state of skyrmions, providing a method for adjusting the channel shape of skyrmions in the field of information transmission.

Acknowledgements

Project supported by the Key-Area Research and Development Program of Guangdong Province, China (Grant No. 2021B0101300003), the Guangdong Basic and Applied Basic Research Foundation, China (Grant Nos. 2022A1515110863 and 2023A1515010837), the National Key Research and Development Program of China (Grant No. 2016YFA0300803), the National Natural Science Foundation of China (Grant Nos. 12304136, 61427812, 11774160, 12241403, 51771127, 52171188, and 52111530143), the Natural Science Foundation of Jiangsu Province, China (Grant Nos. BK20192006 and BK20200307), the Fundamental Research Funds for the Central Universities, China (Grant No. 021014380113), International Exchanges 2020 Cost Share (NSFC), China (Grant No. IEC\NSFC\201296), and the Project for Maiden Voyage of Guangzhou Basic and Applied Basic Research Scheme, China (Grant No. 2024A04J4186).

References

[1] Parkin S S, Hayashi M and Thomas L 2008 *Science* **320** 190
[2] Zhang X, Zhao G P, Fangohr H, Liu J P, Xia W X, Xia J and Morvan F J 2015 *Sci. Rep.* **5** 7643
[3] Fert A, Cros V and Sampaio J 2013 *Nat. Nanotechnol.* **8** 152
[4] Hrabec A, Sampaio J, Belmeguenai M, Gross I, Weil R, Chérif S. M, Stashkevich A, Jacques V, Thiaville A and Rohart S 2013 *Nat. Nanotechnol.* **8** 742
[5] Roessler U. K, Bogdanov A and Pfleiderer C 2006 *Nature* **442** 797
[6] Mühlbauer S, Binz B, Jonietz F, Pfleiderer C, Rosch A, Neubauer A, Georgii R and Böni P 2009 *Science* **323** 915
[7] Münzer W, Neubauer A, Adams T, Mühlbauer S, Franz C, Jonietz F, Georgii R, Böni P, Pedersen B, Schmidt M, Rosch A and Pfleiderer C 2010 *Phys. Rev. B* **81** 041203
[8] Jiang W, Upadhyaya P, Zhang W, Yu G, Jungfleisch M. B, Fradin F Y, Pearson J E, Tserkovnyak Y, Wang K L, Heinonen O, te Velthuis S G E and Hoffmann A 2015 *Science* **349** 283
[9] Zhang S, Wang J, Zheng Q, Zhu Q, Liu X, Chen S, Jin C, Liu Q, Jia C and Xue D 2015 *New J. Phys.* **17** 023061
[10] Li S, Kang W, Huang Y, Zhang X, Zhou Y and Zhao W 2017 *Nanotechnology* **28** 31LT01
[11] Yu G, Upadhyaya P, Shao Q, Wu H, Yin G, Li X, He C, Jiang W, Han X, Amiri P K and Wang K L 2017 *Nano Lett.* **17** 261
[12] Liu Y, Yin G, Zang J, Shi J and Lake R K 2015 *Appl. Phys. Lett.* **107** 152411
[13] Zhang X, Ezawa M, Xiao D, Zhao G, Liu Y and Zhou Y 2015 *Nanotechnology* **26** 225701
[14] Schott M, Bernand-Mantel A, Ranno L, Pizzini S, Vogel J, Béa H, Baraduc C, Auffret S, Gaudin G and Givord D 2017 *Nano Lett.* **17** 3006
[15] Zhang S, Zhang J, Wen Y, Chudnovsky E M and Zhang X 2018 *Appl. Phys. Lett.* **113** 192403
[16] Wang Z, Guo M, Zhou H A, Zhao L, Xu T, Tomasello R, Bai H, Dong Y, Je S G, Chao W, Han H S, Lee S, Lee K S, Yao Y, Han W, Song C, Wu H, Carpentieri M, Finocchio G, Im M Y, Lin S Z and Jiang W 2020 *Nat. Electron.* **3** 672
[17] Song L, Yang H, Liu B, Meng H, Cao Y and Yan P 2021 *J. Magn. Magn. Mater.* **532** 167975
[18] Wang Y, Wang L, Xia J, Lai Z, Tian G, Zhang X, Hou Z, Gao X, Mi W, Feng C, Zeng M, Zhou G, Yu G, Wu G, Zhou Y, Wang W, Zhang X X and Liu J 2020 *Nat. Commun.* **11** 3577
[19] Hou Z, Wang Y, Lan X, Li S, Wan X, Meng F, Hu Y, Fan Z, Feng C, Qin M, Zeng M, Zhang X, Liu X, Fu X, Yu G, Zhou G, Zhou Y, Zhao W, Gao X and Liu J M 2021 *Adv. Mater.* **34** e2107908
[20] Zhang H, Zhang Y, Hou Z, Qin M, Gao X and Liu J 2023 *Materials Futures* **2** 032201
[21] Guang Y, Zhang L, Zhang J, *et al.* 2023 *Adv. Electron. Mater.* **9** 2200570
[22] Yang S, Son J W, Ju T S, *et al.* 2023 *Adv. Mater.* **35** 2208881
[23] Zázvorka J, Jakobs F, Heinze D, *et al.* 2019 *Nat. Nanotechnol.* **14** 658
[24] Yao Y, Chen X, Kang W, *et al.* 2020 *IEEE Trans. Electron Dev.* **67** 2553
[25] Yan Z R, Liu Y Z, Guang Y, Yue K, Feng J F, Lake R K, Yu G Q and Han X F 2021 *Phys. Rev. Appl.* **15** 064004
[26] Wang J, Xia J, Zhang X, Zhao G. P, Ye L, Wu J, Xu Y, Zhao W, Zou Z and Zhou Y 2018 *J. Phys. D: Appl. Phys.* **51** 205002
[27] Hu G, Luo J, Wang J, Lu X, Zhao G, Liu Y, Wu J and Xu Y 2023 *J. Phys. D: Appl. Phys.* **56** 085001

[28] Wang J, Xia J, Zhang X, *et al.* 2020 *Appl. Phys. Lett.* **117** 202401
[29] Tomasello R, Guslienko K Y, Ricci M, *et al.* 2018 *Phys. Rev. B* **97** 060402
[30] Zhao L, Wang Z, Zhang X, *et al.* 2020 *Phys. Rev. Lett.* **125** 027206
[31] Wang J, Strungaru M, Ruta S, Meo A, Zhou Y, Deák A, Szunyogh L, Gavriloaea P I, Moreno R, Chubykalo-Fesenko O, Wu J and Xu Y 2021 *Phys. Rev. B* **104** 054420
[32] Morshed M G, Vakili H and Ghosh A W 2022 *Phys. Rev. Appl.* **17** 064019
[33] Shen L, Xia J, Zhao G, Zhang X, Ezawa M, Tretiakov O A, Liu X and Zhou Y 2019 *Appl. Phys. Lett.* **114** 042402
[34] Luo J, Guo J H, Hou Y H, Wang J L, Xu Y B, Zhou Y, Pong P W T and Zhao G P 2023 *Chin. Phys. Lett.* **40** 097501
[35] Thiele A 1973 *Phys. Rev. Lett.* **30** 230